Published in final edited form as:
Cell Mol Bioeng. 2010 March 1; 3(1): 76–83. doi:10.1007/s12195-010-0106-2.

Rho Kinase Regulation of Fibroblast Migratory Mechanics in Fibrillar Collagen Matrices

Chengxin Zhou and **W. Matthew Petroll**
Biomedical Engineering Program and Department of Ophthalmology, University of Texas Southwestern Medical Center

Abstract

Migration of activated corneal fibroblasts plays an important role in matrix patterning during embryonic development and wound repopulation following injury or refractive surgery. In this study, we investigate the role of Rho kinase in regulating fibroblast migration mechanics, by modifying a previously described nested collagen matrix model to facilitate dynamic imaging of cell-matrix interactions.

Human corneal fibroblasts were cultured in nested matrices with media containing either 1% fetal bovine serum (FBS), or 1% FBS plus the Rho kinase inhibitor Y-27632. Time-lapse DIC imaging of cell and extracellular matrix (ECM) movements was performed for up to 72 hours. In addition, static confocal imaging was used to assess 3-D cell morphology and local matrix reorganization.

In 1% FBS, significant tractional forces were generated during migration, as indicated by inward displacement and reorganization of collagen in front of cells. When Rho kinase was inhibited, cells became more elongated, and extended dendritic processes into the outer matrix. Interestingly, these dendritic cells were still able to generate tractional forces at their leading edge, whereas cell translocation was substantially reduced. Overall, the data suggests that Rho kinase impacts 3-D fibroblast migration by affecting morphology, polarization, and mechanical coordination between the leading and trailing edges of cells.

INTRODUCTION

Migration of activated corneal keratocytes (corneal fibroblasts) is involved in matrix patterning during developmental morphogenesis and is also required for repopulation of corneal tissue following wounding due to injury or surgery.[7, 13] Following lacerating injury or incisional surgery, contractile force generation is needed to facilitate wound closure and prevent loss of the mechanical integrity of the cornea. However, following refractive surgical procedures such as PRK or LASIK, it is preferable to minimize cellular force generation and fibrosis during repopulation, since these alter corneal shape and transparency. Understanding how cell-matrix mechanical interactions are regulated during migration is the first step towards the development of strategies to modulate these aspects of corneal wound healing in vivo.

The Rho-family GTPases, such as Rho and Rac, play a central role in the regulation of cell morphology, cytoskeletal organization and global contraction of 3-D collagen matrices. Rho is known to promote increased phosphorylation of myosin light chain via Rho-kinase (ROCK) inhibition of myosin light chain phosphatase (MLCPase), resulting in increased

Correspondence: W. Matthew Petroll, Ph.D., Department of Ophthalmology, UT Southwestern Medical Center, 5323 Harry Hines Blvd., Dallas, TX 75390-9057, Tel: 214-648-7216, Fax: 214-648-8447, matthew.petroll@utsouthwestern.edu.

actin-myosin II based cell contractility.[1, 14] In time-lapse studies of corneal fibroblasts plated on top or within restrained 3-D collagen matrices, addition of LPA activates Rho, and induces retraction of cell processes and a corresponding pulling in of the surrounding ECM.[18, 20] In contrast, inhibiting ROCK induces rapid cell body elongation, formation and extension of dendritic cell processes, and a corresponding relaxation of cell-induced tension on the matrix.[23] Quantitative analysis of static confocal images has directly demonstrated that when Rho kinase is inhibited, cell-induced matrix reorganization (compaction and alignment of fibrils) is also significantly reduced.[10, 11] However, despite an overall decrease in cellular force generation, both corneal and dermal fibroblasts can still displace the collagen surrounding them when Rho kinase is inhibited.[17, 22] Furthermore, PDGF-induced elongation, ruffling and branching of pseudopodia still occurs in the presence of Y-27632 and/or blebbistatin (which inhibits myosin II), and small tractional forces are generated at the tips of extending processes.[17] The mechanism underlying the generation of these small tractional forces and their role in cell migration is unclear.

Rho Kinase has been shown to facilitate 3-D cell invasion by aligning collagen and inhibiting cell branching thereby facilitating directional persistence.[3, 19] However, the effect of Rho kinase on migration varies depending on cell type and the culture model used.[5, 21] Furthermore, dynamic assessments of cell/matrix interactions in 3-D culture following Rho kinase inhibition have been limited. Thus despite its role in regulating cell contractility and matrix reorganization, the mechanisms through which Rho kinase regulates fibroblast migratory behavior within fibrillar collagen matrices remain unclear.

We recently developed a model for directly investigating cell-matrix mechanical interactions during migration in which cell-seeded compressed collagen matrices are nested within acellular uncompressed matrices.[9] Compressed matrices can be generated rapidly, and have a geometry and mechanical properties similar to in vivo corneal tissue.[2, 12] In this study, we modify this model to facilitate time-lapse imaging, thereby allowing direct visualization of the pattern of cell-matrix interactions during migration. We apply this novel experimental model to study the role of Rho kinase in regulating the mechanics of fibroblast migration in this 3-D model.

METHODS

Cell Culture

A telomerase-infected, extended life-span human corneal fibroblast cell line (HTK) was used.[6] Cells were maintained in “complete media” consisting of Dulbecco’s modified Eagle’s minimum essential medium (DMEM; Invtrogen, Carlsbad, CA) with 1% penicillin/streptomycin amphotericin B (Fungizone; BioWhittaker, Inc., Walkersville, MD) and 10% fetal bovine serum.

Preparation of Nested Collagen Matrices

Rat tail type I collagen was diluted using acetic acid to final concentration of 2.5 mg/ml. 5 ml of the mixture was added to 0.6 ml of 10× DMEM and neutralized with 1 N NaOH. The solution was mixed with 7×10^6 HTK cells in 0.6 ml DMEM, poured into a stainless steal mould, and placed in a incubator for 30 min for polymerization. The polymerized gel was then compacted by compression and blotting, as illustrated in Fig. 1. 6 mm diameter buttons were cut out of this matrix using a trephine. Buttons were placed within acellular, uncompressed collagen matrices (2.5 mg/ml) which had been poured onto Bioptechs culture dishes. For time-lapse experiments, a solution of 2.0 μm diameter carboxylate-modified red fluorescent latex beads (9000 beads/μL, Molecular Probes, Eugene, OR) was mixed with this acellular collagen solution at 1:10 (v/v) ratio prior to polymerization. Constructs were

placed in an incubator for 1 hour to allow polymerization of the outer matrix. The constructs were then overlaid with 1.5 ml of either 10% FBS, 1% FBS or 1%FBS + 10uM Y-27632.

Time-Lapse DIC Imaging

After one hour of incubation, live-cell imaging of constructs was performed using a previously described Nikon TE200 inverted microscope equipped for time-lapse DIC imaging.[16] An environmental chamber (In Vivo Scientific, Valley Park, MO) was used to control temperature, humidity and CO_2 during imaging. At each 20 minute time interval, a z-series of 20X DIC images was collected from the bottom to the top of the construct, at the edge of the inner matrices. This produced a 4-D dataset which captured the cell migration into the outer matrix. Experiments were performed three times for each condition.

F-Actin Labeling and DNA Staining

In other experiments, following 72 hours of culture, constructs were fixed using 3% paraformaldehyde in phosphate buffer for 10 min and permeabilized with 0.5% Triton X-100 in phosphate buffer for 3min. Cells were labeled with Alexa Fluor 488 Phalloidin (1:50; Molecular Probes, Eugene, OR) for 1 hour and then washed in phosphate buffered saline (PBS; 3 times for 5 minutes). Propidium iodide (1:100; Molecular Probes) was then added to each construct to stain the cell nuclei. Constructs were then incubated for 15 minutes and washed with PBS (3 times for 5 minutes).

Laser Confocal Microscopy

Fluorescent (for f-actin and nuclei) and reflected light (for collagen fibrils) 3-D optical section images were acquired using laser confocal microscopy (Leica SP2, Heidelberg, Germany). A HeNe laser (633nm) was used for reflection imaging, and Argon (488 nm) and GreNe (543 nm) lasers was used for fluorescent imaging of phalloidin and propidium iodide (PI), respectively. 3-D optical stacks (z-series) of cells which had migrated into the outer matrix were acquired by changing the position of the focal plane in 10μm steps using a 20X objective (non-immersion, 0.7 NA, 590μm free working distance) or 1μm steps using a 63X objective (water immersion, 1.2 NA, 220μm free working distance).

Cell and Bead Tracking

Time-lapse sequences from a single plane (one z-position) were extracted from the 4-D DIC datasets. In some experiments, there was a shift in the position of the edge of the inner matrix over the course of the experiment. The ‘Align Stack’ tool in MetaMorph software was used to correct for this shift prior to quantitative analysis. Beads in outer matrices were manually tracked using the ‘track points’ module of MetaMorph, and the X-Y coordinates were logged into an Excel file. A custom written “C” program then generated tracks of bead movement over time.[15] To measure cell migration paths, movement of the cell nuclei were tracked using the same procedure. Noise can accumulate when tracking every frame over a long time-lapse experiment, which could reduce the reliability of those results. Thus we instead measured net bead and cell displacements (measured from first and last frames in a sequence) to avoid this issue. Analysis was also limited to beads that were beyond the leading edge of the migration front.

Analysis of Confocal Images

Maximum intensity projection images of PI image stacks were created using Metamorph and overlaid with reflection images. Photoshop was then used to align these overlapped images, resulting in a 750μm wide montage image for each quadrant (Fig. 2). Each montage included the border of the inner matrix (detected by reflected light) and the farthest moving cells. The distance that cells had traveled was calculated by drawing a straight line between

the interface and the leading edge cell nuclei – approximately 5 cells were used from each montage. The number of cells per 750μm wide montage was also counted.

RESULTS AND DISCUSSION

Cell Migration in Serum-Containing Media

We previously developed a nested matrix model in which cell migration and collagen fibril reorganization induced by fibroblast migration was investigated using static confocal imaging.[9] In the current study, we reduced the size of the constructs, and plated them on smaller glass bottom culture dishes appropriate for DIC imaging within a microscope environmental chamber. In our original model, there was a delay of 2–3 days before cells migrated into the outer matrix. Thus we also increased the cell density within the compressed inner matrices (from 1×10^6 to 7×10^6) to facilitate more rapid cell migration into the outer matrix. Using this new model, time-lapse live cell DIC imaging was successfully performed for up to 72 hours without any apparent impact on cell viability.

We first attempted to visualize the migratory process in constructs cultured in media containing 10%FBS. However, cells contracted the inner compressed matrix in 10%FBS, which resulted in inward displacement of the edge (due to the decrease in diameter) and made long-term time-lapse imaging problematic (Movie 1). While serum contains several pro-migratory growth factors (including PDGF), it also contains factors such as lysophosphatidic acid (LPA) and sphingosine-1-phosphate (S1P) which stimulate cell contractility through activation of the Rho/Rho Kinase pathway.[8] Thus to reduce the amount of cellular force generation, we tried a lower serum concentration. Inward movement of the matrix edge was significantly reduced when using 1%FBS, thus this concentration was used for all subsequent time-lapse experiments.

In 1% FBS, fibroblasts began to extend pseudopodial processes into the outer matrices 6–10 hours after plating (Movie 2, Fig. 3A). By 24 hours, many cells had completely escaped the inner matrix (Fig. 3B). Beads in the outer matrix were pulled inward due to cell spreading and migration (Fig 3, red tracks); control experiments without cells did not show any bead movement. By 48 hours, cells were oriented at random angles with respect to the edge of the inner matrix (Fig. 3C); this pattern was more clearly observed in reconstructions of confocal images collected at 72 hours (Fig. 5A). Inspection of time-lapse movies of individual cells revealed significant tractional force generation during migration, as indicated by deformation of the collagen ECM at the leading edge (Movie 3). At the rear, apparent rupture of cell-matrix adhesions resulted in elastic recoil of the tail and release of ECM tension, as indicated by collagen movement away from the cell. Fibroblasts generally assumed an elongated spindle-shaped morphology; however, there were often multiple pseudopodial processes at the leading edge. Cells continuously extended and retracted these processes as they moved into the outer matrix, which resulted in more dynamic behavior than is typically observed on planar substrates (Movie 3).

There was a large degree of variability in the speed and pattern of cell migration observed in 1%FBS. In general, faster moving cells had clear, persistent leading edges with active pseudopodia and a streamline tail (Fig. 4A). Slower migrating cells tended to be less polarized, with both the front and rear exhibiting active pseudopodial processes and associated collagen displacements (Fig. 4B). This “tail plasticity” has also been observed when using micropatterned 1-D substrates to simulate 3-D cell migration.[24]

Effect of Rho Kinase Inhibition

The Rho kinase inhibitor Y-27632 has previously been shown to prevent formation of stress fibers, reduce cell contractility, and inhibit cell-induced matrix reorganization in 3-D

culture.[10, 22] To assess the impact of Rho kinase on the migratory mechanics of corneal fibroblasts, Y-27632 was added to the culture media at the time of plating.

When Rho kinase was inhibited using Y-27632, cells extended thin dendritic processes into the outer matrix (Fig. 6A). During this process, beads in the outer matrix were pulled inward (Movie 4). At 24 hours, cells had only partially escaped the inner matrix (Fig. 6B), and few cells had completely left the inner matrix even after 48 hours. Thus despite rapid extension of processes into the outer matrix, translocation of the cell body appeared to be impaired. All cells maintained numerous thin branching processes (Fig. 6C), which were best appreciated from confocal reconstructions (Fig. 5B). While the pseudopodial processes observed in 1%FBS were generally parallel to the bottom of the dish, the dendritic processes observed following Rho kinase inhibition were more randomly oriented and extended along the z-axis, consistent with previous observations.[10] All quantitative data was obtained using 10 μM Y-27632, which is the standard dosage that provides maximum inhibition with minimal loss of specificity. To assess whether the residual traction might be due to residual Y-27632 activity, a few additional experiments were performed using 50μM Y-27632. A similar response was observed qualitatively. We have also performed experiments using another ROCK inhibitor, fasudil (20 μM, Sigma), which has a different inhibition profile. Fasudil induced a change in cell morphology and apparent reduction in cell migration similar to Y-27632 (Supplemental Figure 1), suggesting the ROCK inhibition is primarily responsible for these effects.

Quantitative analysis confirmed that both the number of cells that migrated into the outer matrix and the distance they traveled was significantly reduced when Rho kinase was inhibited (Fig. 7A). Furthermore, the rate of cell migration decreased following Rho kinase inhibition (Fig. 7B). Interestingly, when the net inward displacements of the beads were compared (i.e. movement perpendicular to the interface), there was no difference between 1% FBS and 1%FBS plus Y-27632 (Fig. 7B). The pattern of bead movement appeared to be more circuitous in 1%FBS, presumably due to the numerous extensions and retractions of pseudopodial processes and the more random pattern of cell alignment. It should be noted that the net inward bead displacements (measured from first and last frames in a sequence being analyzed) were used for quantitative analysis to maximize signal to noise, and this could potentially underestimate total bead movement, particularly in 1% FBS conditions. However, the predominant direction of bead movement was always perpendicular to the interface, thus this error should be low.

A decrease in the amount of local cell-induced matrix reorganization (i.e. compaction and alignment of collagen fibrils) was also observed at 72 hours following Rho kinase inhibition (Fig. 8). This could result from reductions in the number of cells in the outer matrix, and/or the amount of contractile force that each cell generates. For tumor cells invading 3-D matrices, ROCK-dependent collagen alignment at the leading edge provides contact guidance that facilitates local invasion of mammary epithelial cells.[19] ROCK-mediated myosin II contractility has also been shown to inhibit endothelial cell branching, which promotes 3-D ECM invasion by encouraging directional persistence.[4] Studies on corneal fibroblasts have demonstrated that Rho kinase dependent contractile forces are localized to the cell body or at the base of pseudopodial processes.[18, 23] The results of the current study suggest that during fibroblast migration, these contractile forces are responsible for pulling the cell body forward through the collagen matrix following extension of the leading edge. Because of its increased collagen density and stiffness, it is possible that reduced contractility may impair the cells ability to pull themselves free of the inner matrix. However, the rate of migration (as indicated by nuclear translocation) did not change substantially after cells left the inner matrix. Thus the decrease in migration rate is not unique to our model configuration.

As mentioned previously, there was a large amount of variation in cell migration speed in 1%FBS. As shown in Figure 9, this variability was lower following ROCK inhibition. Interestingly, the maximum cell speed was reduced more than the mean cell speed. Thus the inability to achieve a fusiform morphology and/or create and aligned collagen path following ROCK inhibition likely prevents any of the cells from achieving optimal migration conditions. Importantly however, cells were still able to migrate through the collagen ECM when Rho kinase was inhibited, albeit slower (Movie 5). These cells extended dendritic processes at random orientations with respect to the leading edge, and did not exhibit the coordinated mechanical behavior typical of mesenchymal cell migration (extension, contraction, tail retraction). Together, our data suggests that ROCK impacts 3-D migration by affecting morphology, polarization, and mechanical coordination between the leading edge, cell body and trailing edge of corneal fibroblasts.[5]

Supplementary Material

Refer to Web version on PubMed Central for supplementary material.

References

1. Amano M, Ito M, Kimura K, Fukata Y, Chihara K, Nakano T, Matsuura Y, Kaibuchi K. Phosphorylation and activation of myosin by Rho-associated kinase (Rho-kinase). J Biol Chem 1996;271:20246–20249. [PubMed: 8702756]
2. Brown RA, Wiseman M, Chuo CB, Cheema U, Nazhat SN. Ultrarapid engineering of biomimetic materials and tissues: Fabrication of nano- and microstructures by plastic compression. Advanced Functional Materials 2005;15:1762–1770.
3. Fischer DJ, Liliom K, Guo Z, Nusser N, Virag T, Murakami-Murofushi K, Kobayashi S, Erickson JR, Sun G, Miller DD, Tigyi G. Naturally occurring analogs of lysophosphatidic acid elicit different cellular responses through selective activation of multiple receptor subtypes. Mol Pharmacol 1998;54:979–988. [PubMed: 9855625]
4. Fischer RS, Gardel M, Ma X, Adelstein RS, Waterman CM. Local cortical tension by myosin II guides 3D endothelial cell branching. Curr Biol 2009;19:260–265. [PubMed: 19185493]
5. Friedl P, Wolf K. Plasticity of cell migration: a multiscale tuning model. J Cell Biol 2009;1:1.
6. Jester JV, Huang J, Fisher S, Spiekerman J, Chang JH, Wright WE, Shay JW. Myofibroblast differentiation of normal human keratocytes and hTERT, extended-life human corneal fibroblasts. Invest Ophthalmol Vis Sci 2003;44:1850–1858. [PubMed: 12714615]
7. Jester JV, Petroll WM, Cavanagh HD. Corneal stromal wound healing in refractive surgery: the role of myofibroblasts. Prog Retin Eye Res 1999;18:311–356. [PubMed: 10192516]
8. Jiang H, Rhee S, Ho C-H, Grinnell F. Distinguishing fibroblast promigratory and procontractile growth factor environments in 3D collagen matrices. Faseb J. 2008 In Press.
9. Karamichos D, Lakshman N, Petroll WM. An experimental model for assessing fibroblast migration in 3-D collagen matrices. Cell Motil Cytoskeleton 2009;66:1–9. [PubMed: 19061246]
10. Kim A, Lakshman N, Petroll WM. Quantitative assessment of local collagen matrix remodeling in 3-D culture: the role of Rho kinase. Exp Cell Res 2006;312:3683–3692. [PubMed: 16978606]
11. Lee PF, Yeh AT, Bayless KJ. Nonlinear optical microscopy reveals invading endothelial cells anisotropically alter three-dimensional collagen matrices. Exp Cell Res 2009;315:396–410. [PubMed: 19041305]
12. Neel EAA, Cheema U, Knowles JC, Brown RA, Nazhat SN. Use of multiple unconfined compression for control of collagen gel scaffold density and mechanical properties. Soft matter 2006;2:986–992.
13. Netto MV, Mohan RR, Ambrosio R Jr, Hutcheon AE, Zieske JD, Wilson SE. Wound healing in the cornea: a review of refractive surgery complications and new prospects for therapy. Cornea 2005;24:509–522. [PubMed: 15968154]

14. Parizi M, Howard EW, Tomasek JJ. Regulation of LPA-Promoted Myofibroblast Contraction: Role of Rho, Myosin Light Chain Kinase, and Myosin Light Chain Phosphatase. Exp Cell Res 2000;254:210–220. [PubMed: 10640419]

15. Petroll WM, Ma L. Direct, dynamic assessment of cell-matrix interactions inside fibrillar collagen lattices. Cell Motil Cytoskeleton 2003;55:254–264. [PubMed: 12845599]

16. Petroll WM, Ma L, Jester JV. Direct correlation of collagen matrix deformation with focal adhesion dynamics in living corneal fibroblasts. J Cell Sci 2003;116:1481–1491. [PubMed: 12640033]

17. Petroll WM, Ma L, Kim A, Ly L, Vishwanath M. Dynamic assessment of fibroblast mechanical activity during Rac-induced cell spreading in 3-D culture. J Cell Physiol 2008;217:162–171. [PubMed: 18452153]

18. Petroll WM, Ma L, Ly L, Vishwanath M. Analysis of the pattern of subcellular force generation by corneal fibroblasts after Rho activation. Eye Contact Lens 2008;34:65–70. [PubMed: 18180688]

19. Provenzano PP, Inman DR, Eliceiri KW, Trier SM, Keely PJ. Contact guidance mediated three-dimensional cell migration is regulated by Rho/ROCK-dependent matrix reorganization. Biophys J 2008;95:5374–5384. [PubMed: 18775961]

20. Roy P, Petroll WM, Cavanagh HD, Jester JV. Exertion of tractional force requires the coordinated up-regulation of cell contractility and adhesion. Cell Motil Cytoskeleton 1999;43:23–34. [PubMed: 10340700]

21. Sarkar S, Egelhoff TBH. Insights into the roles of non-muscle myosin IIA in human keratinocyte migration. Cell and Mol Bioeng 2009;2:486–494.

22. Tamariz E, Grinnell F. Modulation of fibroblast morphology and adhesion during collagen matrix remodeling. Mol Biol Cell. 2002 In Press.

23. Vishwanath M, Ma L, Otey CA, Jester JV, Petroll WM. Modulation of corneal fibroblast contractility within fibrillar collagen matrices. Invest Ophthalmol Vis Sci 2003;44:4724–4735. [PubMed: 14578392]

24. Wang, YL. Frontiers in Cell Migration. Bethesda, MD: 2008. Exploring the basic principles of cell shape control.

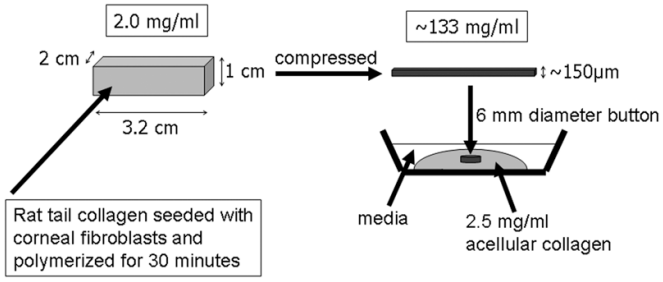

Figure 1.

Method for constructing nested matrix model. (Modified from Kim A, Lakshman N, Karamichos D, Petroll WM. Growth factor regulation of corneal keratocyte differentiation and migration in compressed collagen matrices. *Invest Ophthalmol Vis Sci*)

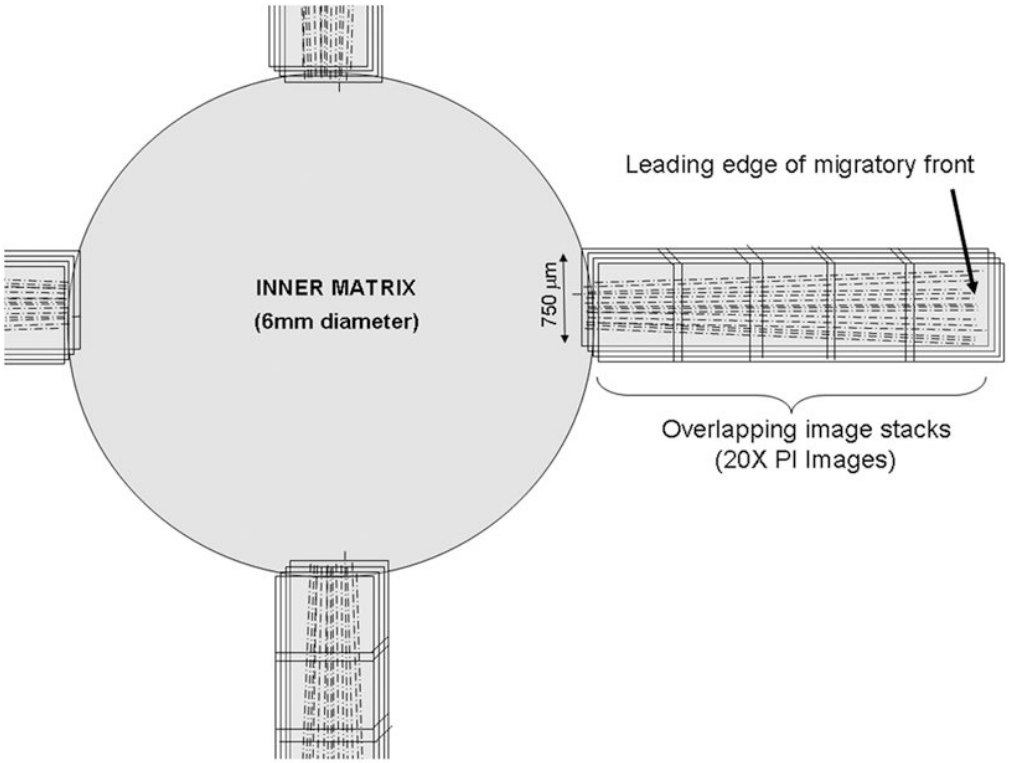

Figure 2.
Schematic showing the montage of 3-D image stacks collected in each sample using laser scanning confocal microscopy. (reproduced from: Karamichos D, Lakshman N, Petroll WM. An Experimental Model for Assessing Fibroblast Migration in 3-D Collagen Matrices. *Cell Motil Cytoskeleton* 66(1):1–9, Copyright © 2009 Wiley-Blackwell)

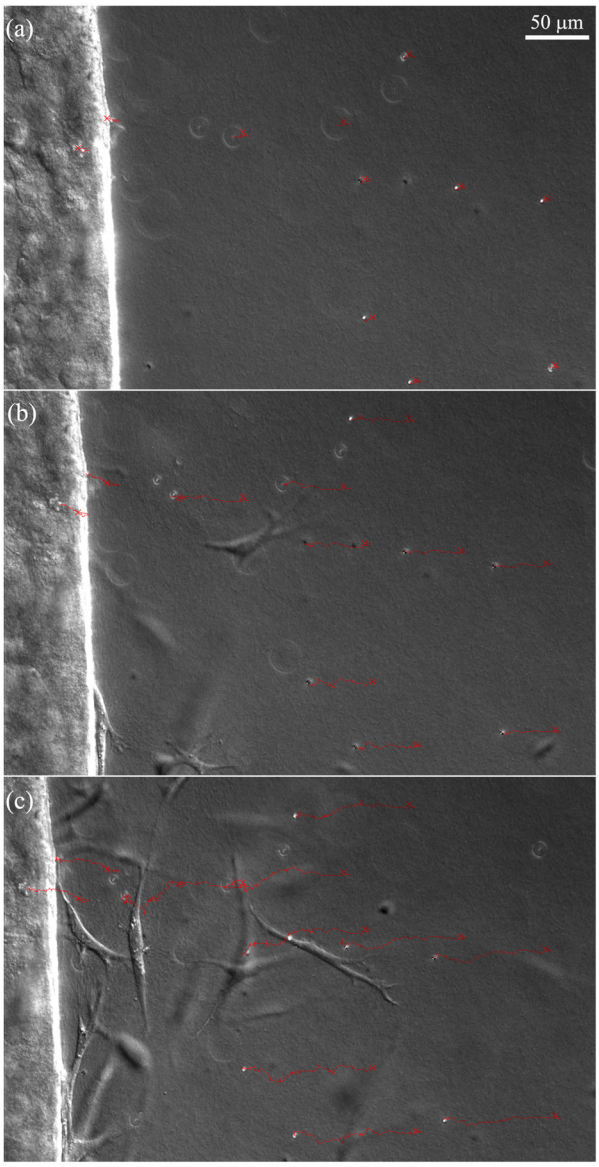

Figure 3.
Time-lapse DIC images collected at 6 hours, 24hours and 48 hours from an experiment in which cells were cultured in 1% FBS. Red tracks show movement of embedded microspheres (crosses mark starting positions). Note that as fibroblasts move out of the inner matrix (left), the beads are pulled inward.

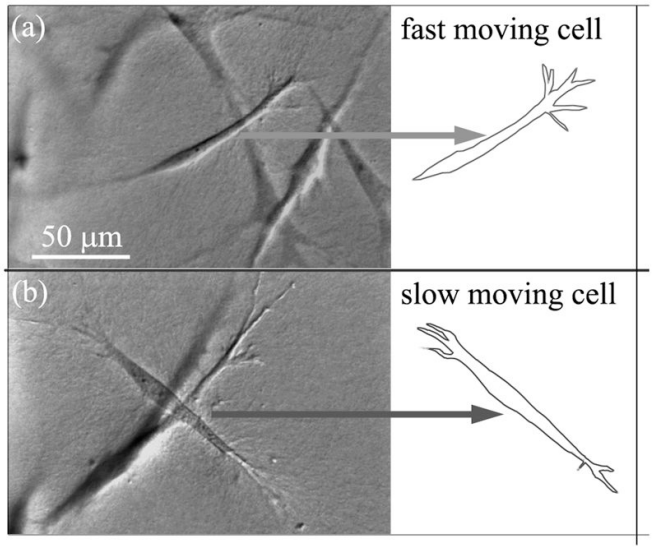

Figure 4.
DIC images of typical fast and slow moving cells in 1%FBS. (A) Fast migrating cell has a clear, persistent leading edge with pseudopodia, and a streamline tail. (B) Slow migrating cell has less distinctive leading and rear edges. Both the front and rear have appreciable pseudopodia.

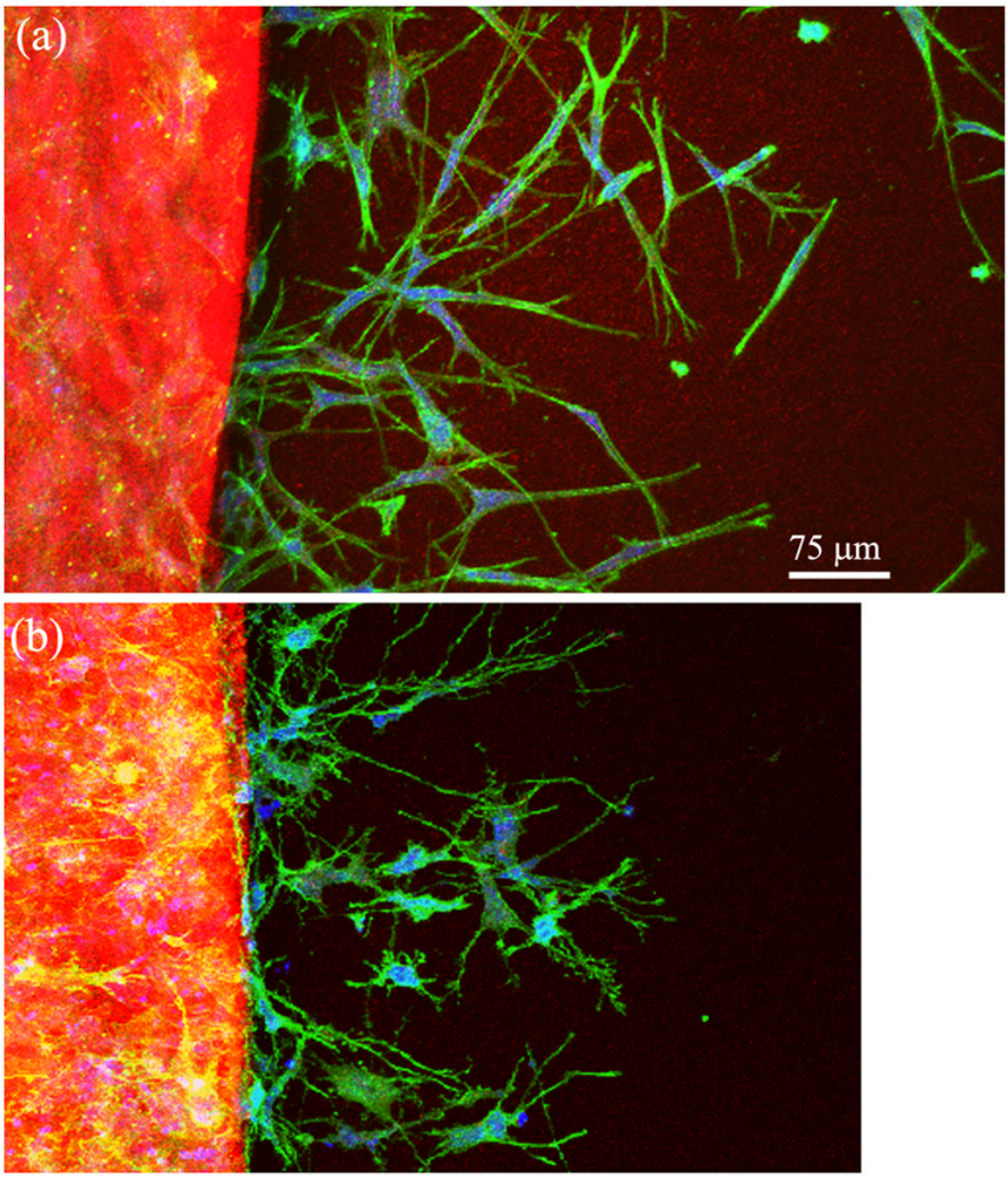

Figure 5.
20X confocal maximum intensity projection images of f-actin (green), collagen fibrils (red) and PI (blue) following 72 hours of culture in (A) 1% FBS, or (B) Y-27632 (10 μM).

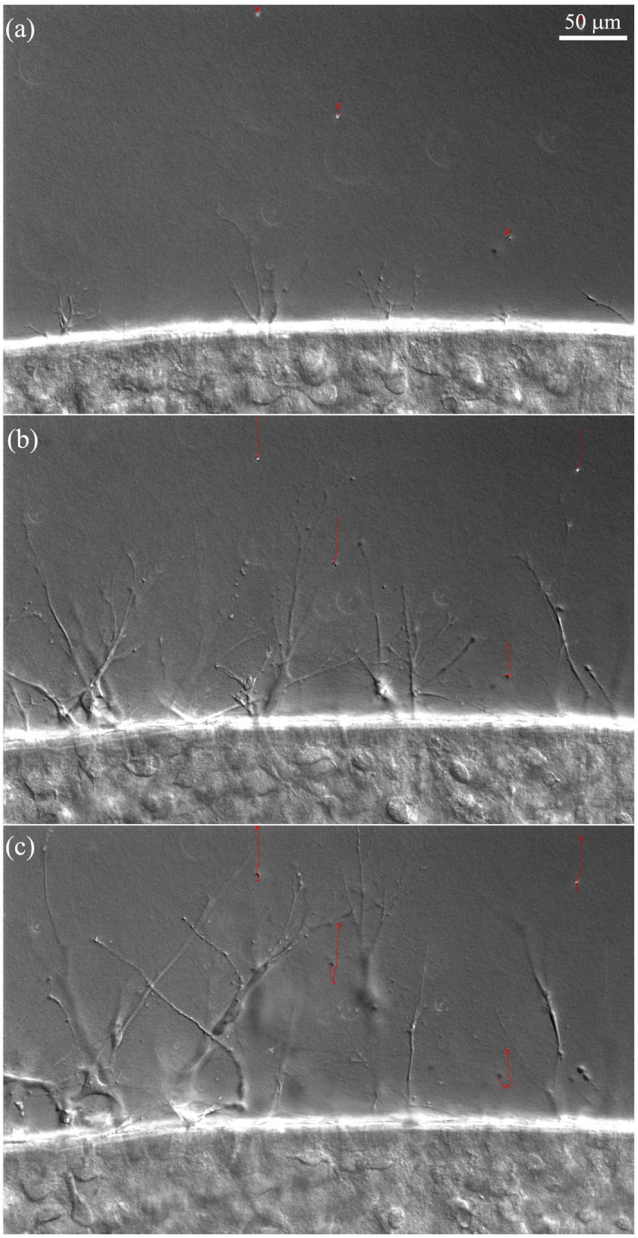

Figure 6.
Time-lapse DIC images collected at 6 hours, 24hours and 48 hours from an experiment in which cells were cultured in 1% FBS + Y-27632. Red tracks show movement of embedded microspheres (crosses mark starting positions). Note that as fibroblasts move out of the inner matrix (bottom), the beads are pulled inward a substantial distance. However, cells assume a more dendritic morphology following Rho kinase inhibition (compare to Figure 3), and take longer to completely escape the inner matrix.

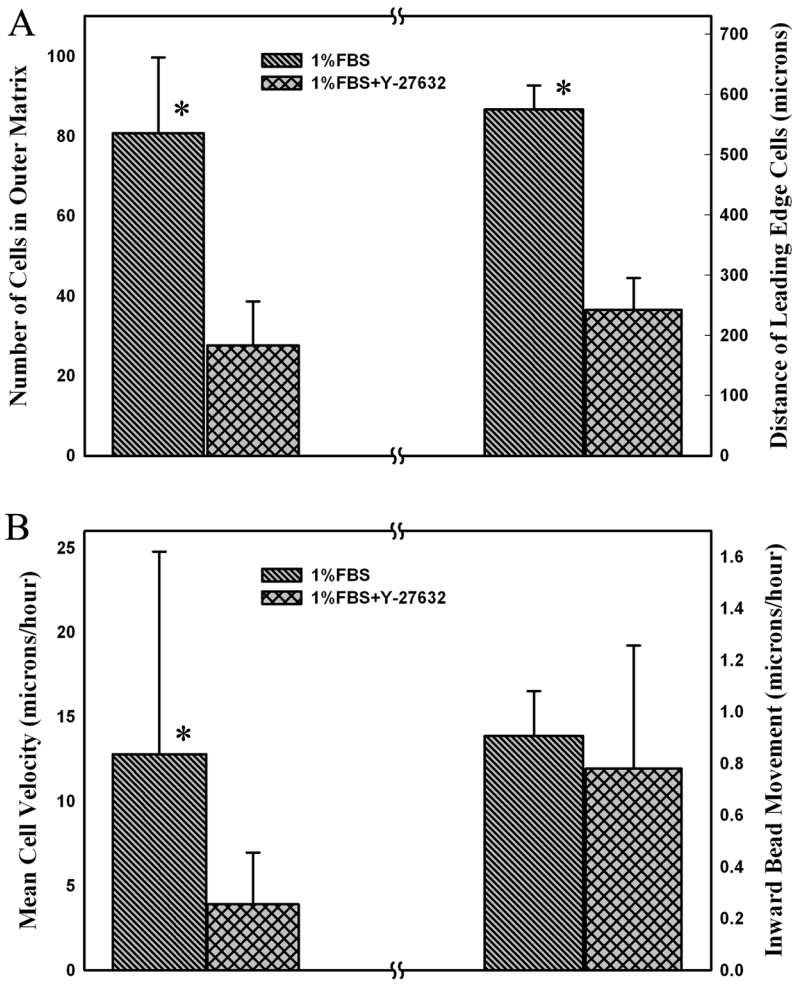

Figure 7.

Quantitative analysis of 72 hour confocal (A) and time-lapse DIC (B) image data. (A) Comparison of number of cell in outer matrix and the distance cells traveled in 1% FBS and 1%FBS plus 10 μM Y-27632. Graphs show mean and standard deviations of 3 constructs per condition. (B) Speed of cell and bead movement under different culture conditions from time-lapse DIC imaging experiments. Inhibiting Rho kinase with Y-27632 significantly reduced the rate of cell movement, but not the net inward bead movement. (Number of cells analyzed was 29 for1% FBS and 19 for 1%FBS plus 10 μM Y-27632. Number of beads analyzed was 15 for1% FBS and 13 for 1%FBS plus 10 μM Y-27632.) * $P < 0.05$.

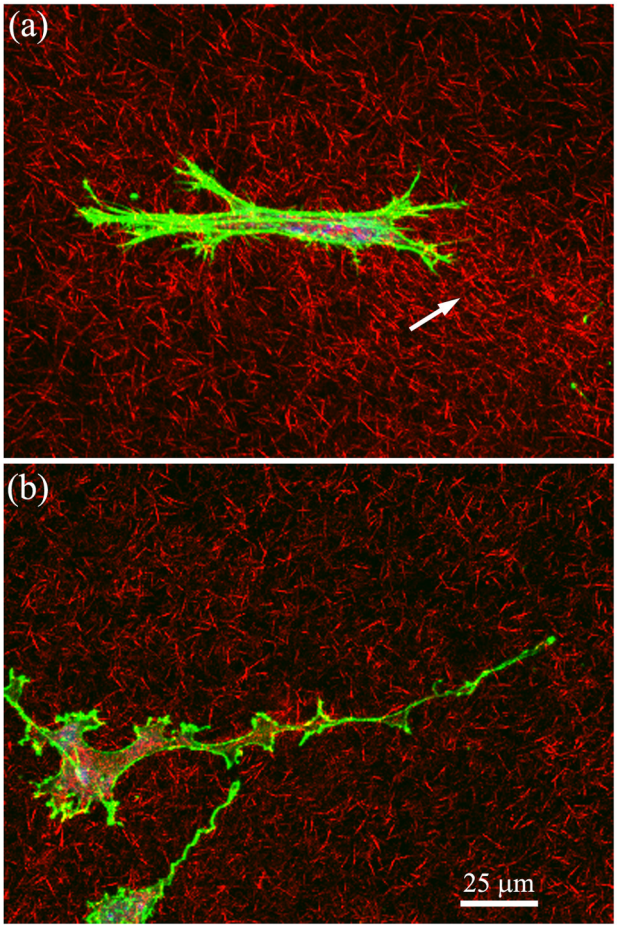

Figure 8.
63X confocal maximum intensity projection images (10 microns thick) of f-actin (green), collagen fibrils (red) and PI (blue) after 3 days of culture. A) Migrating cell near leading edge under 1%FBS condition. Cell is bipolar, and compaction of collagen is observed at one end of the cell (arrow). B) Migrating cell near leading edge under 1%FBS + Y-27632 condition. Cell has an elongated dendritic morphology, and the surrounding ECM is less compacted.

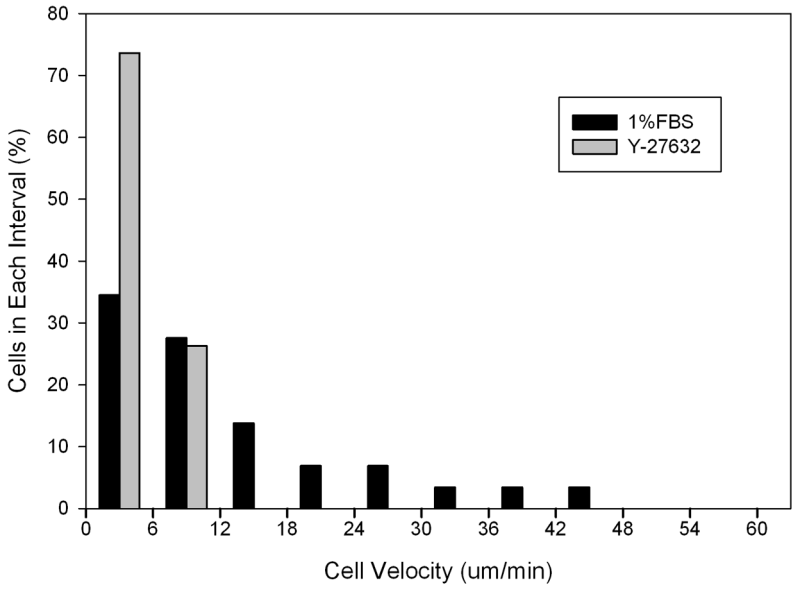

Figure 9.
Histograms of cell velocities under different culture conditions, from time-lapse DIC imaging experiments. Inhibiting Rho kinase with 10 μm Y-27632 dramatically reduced the range of cell velocities.